4-20-2000

Spectroscopic Abundances in Cool Pleiades Dwarfs and NGC 2264 Stars

Jeremy R. King
Clemson University, jking2@clemson.edu

David R. Soderblom
Space Telescope Science Institute

Debra Fischer
San Francisco State University

Burton F. Jones
University of California

THE ASTROPHYSICAL JOURNAL, 533:944–958, 2000 April 20

SPECTROSCOPIC ABUNDANCES IN COOL PLEIADES DWARFS AND NGC 2264 STARS

JEREMY R. KING[1] AND DAVID R. SODERBLOM
Space Telescope Science Institute, 3700 San Martin Drive, Baltimore, MD 21218; jking@stsci.edu, drs@stsci.edu
DEBRA FISCHER
Department of Physics and Astronomy, San Francisco State University, San Francisco, CA 94132; fischer@stars.sfsu.edu
AND
BURTON F. JONES
Board of Studies in Astronomy and Astrophysics, University of California Observatories/Lick Observatory, University of California, Santa Cruz, Santa Cruz, CA 95064; jones@ucolick.org
Received 1999 July 28; accepted 1999 November 30

ABSTRACT

We derive parameters and abundances of several elements in two cool Pleiades dwarfs, four cool NGC 2264 pre–main-sequence stars, and a probable NGC 2264 nonmember from high-resolution, moderate signal-to-noise ratio, Keck/HIRES spectra. Our Pleiades Fe abundance agrees with previous spectroscopic and photometric values of hotter stars and does not resolve the 0.3 mag distance modulus discrepancy between main-sequence fitting and *Hipparcos* parallaxes. Abundances of Cr-Ca-Ti-Al are subsolar, mimicking the pattern of interstellar medium abundances. While modest temperature errors may contribute, the results (particularly for Al) could suggest an association with ionization potential; such effects might be related to the Pleiades Li scatter. The cluster Fe scatter and its relation to Li scatter is discussed. Three NGC 2264 members suggest [Fe/H] = −0.15 and near-solar ratios of other elements. Mildly supersolar abundances for another object support its probable nonmembership. A fourth member exhibits an Mg-Si-Fe-Ni and Cr-Ti-Ca-Al dichotomy opposite to that of the Pleiades stars; a relation to ionization potential is again suggested. A 0.15–0.20 dex scatter or steep decline, neither well accommodated by stellar models, in the NGC 2264 Li abundances with $T_{\rm eff}$ is indicated. We note the surprising presence of the λ7774 O I triplet in our Pleiades stars, one of the cool NGC 2264 stars, and the K6 field dwarf GL 241. The inferred LTE O abundances are enhanced by 0.23–0.85 dex over solar, suggesting that even non-LTE calculations of the O I triplet are incomplete and perhaps implicating the influence of an overlying chromosphere. Our results demonstrate the utility of cluster abundances besides Fe and Li in addressing fundamental issues concerning stellar evolution and systematic errors in the analysis of cool young stars.

Subject headings: open clusters and associations: individual (NGC 2264, Pleiades) — stars: abundances — stars: atmospheres — stars: late-type — stars: pre–main-sequence

1. INTRODUCTION

As assemblages of stars of varying mass but common history, open clusters are valuable probes of stellar physics and Galactic evolution. Important relevant parameters are the "metal" abundances of the cluster stars. These abundances are of specific interest for several reasons. First, they are fundamental to exploration of Galactic structure and evolution via constraints provided by cluster age-metallicity relations and spatial metallicity gradients (e.g., Twarog, Ashman, & Anthony-Twarog 1997).

Second, open cluster star metallicities are important for constraining stellar physics, which has important implications for diverse issues such as the universal age and the primordial Li abundance. Recent work demonstrates the importance of open cluster abundances for stellar evolution in three different contexts. First, ages of the oldest open clusters set a lower age to that of the Galactic disk; cluster metallicity is an important parameter in age determinations from theoretical isochrones (Demarque, Green, & Guenther 1992). Second, as has been recently emphasized by Randich et al. (1997) and Chaboyer, Demarque, & Pinsonneault (1995, hereafter CDP95), metallicities are important parameters in constraining stellar models using open cluster main-sequence Li-$T_{\rm eff}$ morphologies. Swenson et al. (1994) have called attention to the potential importance of abundances of elements besides Fe in interpreting cluster Li observations in terms of stellar models. Third, Pinsonneault et al. (1998) and Soderblom et al. (1998) have recently considered the 0.3 mag discrepancy between the Pleiades distance modulus derived from main-sequence fitting and from *Hipparcos* parallaxes. If this fundamental discrepancy is not due to systematic errors in the parallaxes, then a fundamental failure in our understanding of stellar evolution is suggested unless abundances in the Pleiades are vastly different than presently believed. Unfortunately, little is known about the abundances of elements other than Li and Fe in even the most well-studied open clusters.

Third, independent determinations of cluster metal abundances derived from data of a variety of stars and using different approaches provide a way to assess the confidence with which we can derive stellar abundances. For example, abundances derived from cluster stars spanning a range in evolutionary state (e.g., giants, F dwarfs, K dwarfs) provide an evaluation of the relative adequacy of model atmospheres, $T_{\rm eff}$ calibrations, and other assumptions. Such tests would be particularly interesting for pre–main-sequence (PMS) stars, but even less is known about detailed abundances of numerous elements in these stars than in well-

[1] Current address: Department of Physics, University of Nevada, Las Vegas, 4505 South Maryland Parkway, Las Vegas, NV 89154-4002.

TABLE 1

MODEL ATMOSPHERE PARAMETERS AND ADOPTED UNCERTAINTIES

Star	$T_{\rm eff}$ (K)	log g (cgs)	ξ (km s^{-1})	[M/H]
HII 676.....	4410 ± 75	4.60 ± 0.15	1.00 ± 0.25	0.05 ± 0.15
HII 97.....	4525 ± 75	4.60 ± 0.15	0.90 ± 0.25	0.05 ± 0.15
J407.....	4660 ± 90	3.83 ± 0.50	1.40 ± 0.25	−0.10 ± 0.15
J428.....	4300 ± 90	3.91 ± 0.50	2.05 ± 0.25	−0.25 ± 0.15
J680.....	4250 ± 90	4.10 ± 0.50	1.95 ± 0.25	−0.10 ± 0.15
J682.....	4570 ± 90	3.45 ± 0.50	2.15 ± 0.25	−0.70 ± 0.15
J1088	5875 ± 90	4.50 ± 0.25	1.55 ± 0.25	0.05 ± 0.15
Sun	5770	4.44	1.10	0.00

studied open clusters. Finally, the very way in which we measure metallicity—in proportion to the Sun—is not just because we can determine solar abundances on an absolute basis. We are also naturally curious about how our Sun compares to the other stars around us.

In previous work, we have utilized high-resolution, moderate signal-to-noise ratio (S/N) spectra obtained with the Keck I 10 m telescope and its HIRES spectrograph to determine Li abundances in solar-type stars of several open clusters. These echelle data also contain considerable information on the abundances of other elements. Here we take a first step toward exploiting this information and addressing some of the above issues. A natural starting point is the Pleiades, a cluster of fundamental importance and having previous abundance analyses. The Pleiades abundances provide a good check on our analysis procedure and results, which we then apply to the more challenging PMS NGC 2264 stars. Our results are some of the first abundances of elements other than Fe and Li in PMS field or cluster stars.

We emphasize that the analysis has focused on quality rather than quantity. We have analyzed only those data which would yield the most reliable abundance determinations from which to draw conclusions. For the Pleiades, we have confined ourselves to the two slowest rotating K dwarfs from the data set summarized below. This is done to derive the most reliable abundances possible for an important comparison of our initial results with previous work. Restricting ourselves to the slowest rotators does not just minimize uncertainties in the line strengths due to photon noise. More important is that even modest rotation makes many of the lines in our cool ($T_{\rm eff} \sim 4500$) dwarfs unusable because of the effects of blending; we also wish to avoid any systematic errors caused by unrecognized effects of blending. Even more restrictive criteria were mandated for the PMS NGC 2264 data. These spectra have lower S/Ns than those for the Pleiades; we believed only the higher S/N spectra were suitable for the present purpose. From the surviving slowly rotating objects having sufficient S/N, we eliminated those which were suspected of being a double-lined spectroscopic binary (SB2) (to avoid the effects of dilution and blending) and those evincing strong Hα emission (to avoid the effects of veiling). This left four certain NGC 2264 members that we could analyze; in addition, one suspected nonmember was purposefully included to see if this could be confirmed from the abundances. The objects are listed in the first column of Table 1.

2. OBSERVATIONAL DATA

Spectra of the cool Pleiades dwarfs HII 97 and HII 676 are those described in Jones et al. (1996, hereafter JSFS). Spectra of the cool NGC 2264 stars J407, J428, J680, J682, and J1088 are those described in Soderblom et al. (1999; their Table 1 provides cross-identifications). The data were acquired with the HIRES echelle spectrograph on the Keck I 10 m telescope and have a ~3 pixel resolving power of ~45,000. The typical per-pixel S/N ratio is 70 for the Pleiades stars and 45–75 for the NGC 2264 stars. These values are modest but wholly adequate for our analysis (perhaps marginally so for J680). We use daytime sky spectra obtained with the same instrumentation during the same programs as solar proxy data. These spectra are much higher quality; the Poisson-based per-pixel S/N is typically near ~700. Portions of the spectra can be seen in Figure 1 of JSFS and Soderblom et al. (1999).

3. ABUNDANCE ANALYSIS

3.1. *Features, Atomic Data, and Line Strengths*

Nearly all the atomic lines used in our analysis were selected from the extensive solar list of Thévenin (1990). The vast majority are the allegedly clean "case *a*" lines. We first considered the effects of possible blends, irrespective of whether a line was classified as a "case *a*" feature, by inspecting the profiles from our high-S/N solar proxy spectrum and the very high resolution solar flux atlas of Kurucz et al. (1984). Because the extent of blending in our cool stars may be quite different, the Pleiades spectra were also inspected for obvious serious blending or problematic asymmetries. Such features found in either the two Pleiades stars or the Sun were eliminated from consideration in the analysis. Lines possibly significantly contaminated by telluric absorption or substantially in the wings of deep Hα absorption were also excluded.

The species and wavelengths of the features used here are listed in the first two columns of Table 2 and are taken from Thévenin (1990). Lower excitation potential and oscillator strengths are from the same source and are listed in the third and fourth columns.[2] These *gf*-values are solar oscillator strengths, i.e., they are derived by an inverse analysis of a specific solar spectrum via specific adopted solar abundances and a specific model atmosphere. Because we cannot adopt identical assumptions here (e.g., *stellar* model atmospheres that are internally consistent with the *solar* atmosphere used by Thévenin do not exist), a differential analysis with respect to the Sun is performed to yield abundances free from uncertainties in simply adopting *gf*-values and solar abundances. Our derived abundances are thus normalized with a consistently determined solar abundance and are *gf*-independent to the extent that we believe the solar oscillator strengths are plausible enough not to produce significant errors from differential curve-of-growth effects.

3.2. *Equivalent Widths and Abundances*

Equivalent widths of the selected lines in our stellar and solar spectra were measured using routines in the one-dimensional spectrum analysis package SPECTRE (Fitzpatrick & Sneden 1987). To attempt determining yttrium abundances, the very weak solar λ6435 Y I feature had to be measured from the Kurucz et al. (1984) solar flux

[2] Atomic data for the $\lambda\lambda$8712, 8717 Mg I lines are taken from Edvardsson et al. (1993); that for the $\lambda\lambda$6318, 7691 Mg I lines is taken from Chang & Tang (1990) and King et al. (1998).

TABLE 2

EQUIVALENT WIDTHS AND ABUNDANCES

						J676		J97		J407		J428		J680		J682		J1088	
ION	λ (Å)	χ (eV)	log *gf*	EW ($_\odot$)	log *N*	EW	[M/H]	EW	[M/H]	EW	[M/H]	EW	[M/H]	EW	[M/H]	EW	[M/H]	EW	[M/H]
Fe I...	6302.50	3.69	−1.16	92.8	7.57	...	...	...	...	126.3	−0.18	128.0	−0.42	...	...	134.5	−0.57	107.0	+0.11
	6311.50	2.83	−3.21	28.6	7.55	...	...	...	...	69.7	0.02	65.3	−0.21	70.2	−0.03	57.5	−0.58	...	...
	6315.81	4.07	−1.76	38.5	7.52	...	...	...	...	60.2	−0.09	53.7	−0.22	52.0:	−0.13	52.3	−0.54	44.6	0.12
	6322.69	2.59	−2.40	74.7	7.43	...	...	...	...	117.5	−0.17	...	...	128.8	−0.29	123.3	−0.67	82.1	0.04
	6330.85	4.73	−1.32	33.3	7.60	...	...	...	...	41.6	−0.19	...	...	...	...	36.5	−0.52	41.9	0.17
	6338.88	4.79	−1.06	48.0	7.68	...	...	...	...	...	...	...	...	...	...	50.8	−0.56	52.3	0.06
	6344.16	2.43	−2.93	58.1	7.47	...	...	...	...	112.7	0.06	...	...	...	...	105.8	−0.62	...	...
	6380.75	4.19	−1.44	50.3	7.54	...	...	...	...	71.8	−0.10	...	...	...	...	48.6	−0.79	53.6	0.04
	6475.63	2.56	−2.97	57.9	7.63	109.3	0.16	109.5	0.19	107.6	0.00	109.0	−0.31	117.1	−0.10	95.4	−0.73	67.1	0.12
	6481.87	2.28	−3.01	67.0	7.57	118.2	0.03	107.1	−0.05	108.5	−0.22	115.1	−0.50	118.4	−0.35	108.9	−0.80	73.5	0.05
	6496.47	4.79	−0.65	63.4	7.53	78.7	0.04	85.0	0.07	79.0	−0.11	65.9	−0.30	72.1:	−0.11	50.0	−0.84	71.0	0.07
	6498.94	0.96	−4.70	46.3	7.51	110.9	0.10	115.8	0.25	110.4	−0.09	...	...	141.9:	−0.07	117.0	−0.65	45.4	0.02
	6533.94	4.56	−1.38	50.4	7.82	...	...	...	...	49.5	−0.39	47.0	−0.40	...	...	35.0:	−0.91	45.3	−0.10
	6581.22	1.48	−4.82	20.8	7.61	58.6	−0.05	69.0	0.18	55.8	−0.35	83.7:	−0.21	...	...	71.3	−0.56	23.2	0.13
	6593.88	2.43	−2.34	86.7	7.43	155.1	0.00	155.7	0.04	...	...	164.6	−0.29	164.4	−0.20	139.6	−0.74	96.8	0.05
	6608.04	2.28	−4.02	18.2	7.53	49.0	0.07	46.5	0.03	47.6	−0.23	62.0	−0.16	74.2	0.13	...	...	17.1	0.03
	6609.12	2.56	−2.67	68.0	7.51	111.2	−0.01	110.1	0.01	116.1	−0.07	...	...	128.8	−0.15	109.9	−0.73	73.9	0.04
	6627.56	4.55	−1.59	28.0	7.58	32.0	−0.01	36.4	0.03	36.7	−0.19	22.1	−0.43	...	...	31.9	−0.53	31.7	0.09
	6703.58	2.76	−3.13	38.3	7.59	74.1	0.12	72.4	0.11	81.4	−0.01	87.5	−0.14	86.4	−0.03	71.9	−0.61	41.2	0.07
	6710.32	1.48	−4.90	16.7	7.56	51.8	−0.05	47.6	−0.10	66.9	−0.05	69.7	−0.27	73.5	−0.11	...	...	21.6	0.21
	6725.36	4.10	−2.30	18.7	7.61	25.7	0.01	26.2	−0.02	29.5	−0.19	21.8:	−0.32	...	...	13.7	−0.85	19.9	0.07
	6726.67	4.61	−1.12	48.8	7.57	59.9	0.06	69.0	0.13	66.7	−0.07	...	...	48.1	−0.21	43.6	−0.73	46.0	−0.06
	6733.15	4.64	−1.52	28.3	7.59	33.8	0.05	39.8	0.11	32.4	−0.26	...	...	...	...	28.1	−0.59	33.3	0.12
	6739.52	1.56	−4.98	11.9	7.54	39.5	−0.07	47.2	0.10	44.1	−0.23	47.0	−0.37	46.4	−0.27	39.6	−0.67	...	...
	6750.16	2.42	−2.48	73.6	7.29	126.7	0.02	117.0	−0.05	117.1	−0.20	135.4	−0.34	...	...	108.2	−0.90	88.6	0.17
	6786.86	4.19	−2.01	27.1	7.62	...	...	...	...	48.2	−0.02	40.0	−0.14	...	...	37.3	−0.49	22.4	−0.08
	6793.27	4.07	−2.48	13.6	7.59	...	...	...	...	27.7	−0.07	...	...	...	...	...	...	21.2	0.27
	6804.01	4.65	−1.92	24.6	7.91	...	...	...	...	38.0	−0.06	14.9:	−0.32	...	...	...	...	23.1	−0.01
	6804.30	4.58	−1.68	16.7	7.38	...	...	...	...	20.9	−0.23	...	...	...	...	18.1	−0.53	19.0	0.10
	6806.86	2.73	−3.24	34.4	7.58	...	...	...	...	79.8	0.04	80.9	−0.15	87.4:	0.06	77.5:	−0.46	40.9	0.15
	6810.27	4.61	−1.12	48.8	7.57	...	...	...	...	...	...	...	...	...	...	...	...	...	...
	6820.37	4.64	−1.27	41.4	7.61	...	...	...	...	55.6	−0.10	...	...	...	...	34.0:	−0.74	50.5	0.15
	6828.60	4.64	−0.94	59.2	7.60	76.1	0.09	86.3	0.16	76.6	−0.09	...	...	...	...	68.5	−0.54	65.8	0.07
	6839.84	2.56	−3.47	33.8	7.63	72.1	0.14	65.7	0.05	61.5	−0.30	...	...	71.9	−0.19	64.0	−0.67	32.2	0.00
	6843.65	4.55	−0.98	63.5	7.63	71.0	−0.06	74.2	−0.06	76.4	−0.18	74.1:	−0.24	...	...	...	...	68.8	0.04
	6858.15	4.61	−1.09	52.2	7.59	61.4	0.03	65.9	0.04	61.3	−0.21	72.1	−0.06:	...	...	38.2:	−0.87	57.0	0.05
	7000.62	4.14	−2.24	18.3	7.56	27.0	0.08	27.6	0.05	29.3	−0.16	19.4:	−0.34	...	...	...	...	...	...
	7212.44	4.95	−1.20	36.0	7.71	...	...	...	...	33.7	−0.32	34.2	−0.21	34.5:	−0.08	...	...	...	...
	7219.68	4.07	−1.69	48.1	7.59	61.8	0.03	69.3	0.11	72.7	−0.05	66.8	−0.18	64.6	−0.09	57.8	−0.63	50.9	0.04
	7351.11	4.99	−1.05	35.7	7.58	...	...	...	...	52.7	0.05	...	...	...	...	...	...	44.3	0.16
	7351.52	4.95	−0.90	44.4	7.56	...	...	...	...	67.1	0.10	...	...	...	...	49.4	−0.45	49.2	0.07
	7401.69	4.19	−1.69	41.8	7.58	47.2	−0.05	53.5	0.01	48.9	−0.31	41.4:	−0.40	40.7	−0.29	52.1	−0.56	42.3	0.01

TABLE 2—*Continued*

Ion	λ (Å)	χ (eV)	log *gf*	EW ($_\odot$)	log *N*	J676		J97		J407		J428		J680		J682		J1088	
						EW	[M/H]	EW	[M/H]	EW	[M/H]	EW	[M/H]	EW	[M/H]	EW	[M/H]	EW	[M/H]
	7443.03	4.19	−1.83	39.3	7.67	44.0	−0.05	46.7	−0.05	52.8	−0.19	37.0	−0.43	38.9	−0.27	37.8	−0.74	42.9	0.07
	7507.27	4.41	−1.18	58.0	7.57	…	…	…	…	80.1	−0.05	71.4	−0.20	78.3:	0.01	…	…	62.7	0.04
	7531.15	4.37	−0.59	96.4	7.56	135.3	0.05	123.5	−0.07	121.2	−0.14	114.3	−0.34	121.0	−0.17	…	…	109.7	0.09
	7568.91	4.28	−0.99	84.0	7.70	113.3	0.03	123.4	0.09	105.5	−0.16	111.4	−0.22	99.4	−0.23	86.1	−0.83	…	…
	7583.80	3.02	−1.96	87.0	7.53	128.5	−0.09	134.8	−0.02	124.0	−0.23	…	…	…	…	…	…	94.1	0.01
	7710.37	4.22	−1.22	71.9	7.66	92.5	0.03	101.5	0.10	96.4	−0.09	86.0	−0.31	101.6	−0.02	78.4:	−0.73	83.5	0.11
	7723.21	2.28	−3.59	48.9	7.71	83.5	−0.05	80.6	−0.06	78.6	−0.38	…	…	95.1	−0.27	89.3	−0.71	57.8	0.14
	7745.52	5.08	−1.29	23.6	7.62	20.6	−0.01	34.3	0.22	39.3	0.10	…	…	…	…	11.6:	−0.81	22.9	0.01
	7746.60	5.06	−1.39	19.8	7.60	24.1	0.18	26.8	0.17	35.7	0.13	…	…	15.2	−0.12	…	…	21.6	0.08
	7912.87	0.86	−4.90	51.3	7.60	127.8	0.15	121.4	0.15	…	…	…	…	…	…	123.4	−0.73	44.2	−0.09
Ni I	6327.60	1.68	−3.23	38.2	6.36	…	…	…	…	72.6	−0.14	91.4	−0.12	65.1	−0.35	63.2	−0.77	42.5	0.11
	6339.12	4.15	−0.70	47.9		…	…	…	…	…	…	…	…	…	…	51.3:	−0.52	50.2	0.02
	6378.26	4.15	−1.00	31.4	6.41	…	…	…	…	32.9	−0.21	…	…	…	…	27.8	−0.59	…	…
	6482.81	1.93	−2.97	42.4	6.43	68.1	0.05	63.0	−0.01	79.5	−0.05	79.8	−0.28	73.6	−0.24	79.0	−0.59	43.2	0.03
	6532.88	1.93	−3.47	17.7	6.35	…	…	…	…	36.2	−0.24	…	…	…	…	…	…	…	…
	6586.32	1.95	−2.95	45.2	6.48	68.9	0.02	67.6	0.01	75.6	−0.17	90.6:	−0.19	86.3	−0.12	67.4	−0.79	46.2	0.02
	6598.61	4.23	−1.02	27.9	6.41	21.4	−0.03	26.8	0.04	37.5	−0.01	…	…	…	…	15.8	−0.79	25.0	−0.05
	6842.04	3.66	−1.52	29.8	6.40	28.0	−0.01	28.0	−0.06	38.4	−0.14	…	…	26.2	−0.19	23.4	−0.76	32.6	0.08
	7001.55	1.93	−3.62	12.9	6.31	29.3	0.09	22.3	−0.08	35.1	−0.09	24.6:	−0.37	…	…	15.9	−0.89	12.0	0.03
	7062.98	1.95	−3.55	15.6	6.36	28.5	−0.03	…	…	38.4	−0.13	30.5	−0.34	…	…	…	…	23.9	0.29
	7122.21	3.54	−0.05	115.0	6.28	129.6	−0.15	132.6	−0.14	124.4	−0.30	115.2	−0.57	…	…	123.6	−0.81	120.5	−0.02
	7385.24	2.74	−2.07	45.1	6.33	53.4	−0.03	55.0	−0.02	61.3	−0.22	54.5	−0.39	56.7	−0.23	51.3	−0.79	46.8	0.03
	7393.61	3.61	−0.04	96.2	6.06	109.0	−0.05	101.2	−0.16	121.0	−0.07	107.4:	−0.37	101.4	−0.32	99.9	−0.82	96.3	−0.10
	7414.51	1.99	−2.44	74.8	6.52	98.9	−0.10	95.8	−0.12	107.9	−0.21	99.9	−0.62	…	…	…	…	…	…
	7422.29	3.63	−0.01	99.5	6.09	108.0	−0.10	118.0	−0.03	109.7	−0.25	116.7:	−0.31	…	…	87.9:	−1.01	104.3	−0.03
	7522.78	3.66	−0.56	83.5	6.41	86.2	−0.08	93.0	−0.03	101.4	−0.10	98.0	−0.25	85.6	−0.27	75.5:	−0.91	93.3	0.05
	7525.12	3.63	−0.69	74.7	6.36	87.9	0.09	78.7	−0.05	84.2	−0.21	78.8	−0.34	83.3	−0.15	70.2	−0.84	85.6	0.09
	7555.61	3.85	0.06	94.8	6.14	101.2	−0.05	103.7	−0.06	99.9	−0.26	110.9	−0.22	87.0	−0.37	78.4	−0.99	94.1	−0.11
	7574.10	3.83	−0.63	66.1	6.33	69.0	0.05	64.7	−0.06	63.8	−0.33	66.5	−0.28	…	…	61.4	−0.75	64.6	−0.08
	7714.31	1.93	−1.80	105.0	6.33	152.9	−0.10	140.5	−0.17	146.6	−0.25	…	…	…	…	154.4	−0.78	…	…
	7715.59	3.70	−1.14	53.0	6.47	50.0	−0.01	47.1	−0.11	53.3	−0.30	43.8	−0.40	46.7:	−0.23	53.3	−0.66	60.5	0.10
	7727.62	3.68	−0.15	92.0	6.14	108.7	0.04	109.7	−0.02	106.5	−0.17	…	…	95.0:	−0.28	87.6	−0.88	107.4	0.12
	7748.89	3.70	−0.18	86.7	6.10	103.8	0.08	111.2	0.13	92.1	−0.27	97.7:	−0.28	…	…	101.4	−0.61	95.0	0.03
Fe II	6416.93	3.89	−2.86	40.3	7.69	…	…	…	…	…	…	…	…	…	…	…	…	42.8	−0.01
	6432.68	2.89	−3.85	40.5	7.72	…	…	…	…	…	…	…	…	…	…	…	…	45.0	0.04
	6456.39	3.90	−2.25	61.6	7.56	…	…	…	…	…	…	…	…	…	…	…	…	76.2	0.15
Cr I	6330.10	0.94	−2.99	27.4	5.77	…	…	…	…	99.2	−0.20	155.5	−0.19	142.3	−0.30	124.6	−0.30	32.5	0.16
	6605.57	4.14	−0.81	9.2	6.11	…	…	…	…	…	…	…	…	…	…	22.3	−0.26	…	…
	6661.08	4.19	−0.24	14.0	5.80	…	…	…	…	49.5	0.16	49.2	−0.05	…	…	29.1	−0.32	22.8	0.28
	6978.48	3.46	0.01	60.3	5.84	133.9	−0.08	128.9	−0.06	123.4	0.06	138.6	−0.25	151.8	−0.12	132.0	−0.17	70.6:	0.13
	6979.81	3.46	−0.46	38.4	5.91	92.3	−0.07	89.8	−0.04	80.4	−0.12	96.4:	−0.30	105.1:	−0.16	86.1	−0.32	46.6:	0.16
	6980.91	3.46	−1.12	10.2	5.81	39.5	−0.02	34.7	−0.07	32.7	−0.15	43.7:	−0.18	53.7	0.00	…	…	…	…

TABLE 2—*Continued*

Ion	λ (Å)	χ (eV)	log *gf*	EW ($_\odot$)	log *N*	J676		J97		J407		J428		J680		J682		J1088	
						EW	[M/H]	EW	[M/H]	EW	[M/H]	EW	[M/H]	EW	[M/H]	EW	[M/H]	EW	[M/H]
Ti I	6303.77	1.44	−1.62	7.8	4.99	...	...	...	...	62.3	−0.03	91.8:	−0.24	106.6	−0.05	75.5	−0.12	5.7	−0.07
	6336.11	1.44	−1.68	10.2	5.18	...	...	...	...	55.2	−0.28	73.2	−0.60	...	...	52.6	−0.54	9.3	0.03
	6508.15	1.43	−2.03	2.7	4.90	42.6	−0.05	34.7	−0.08	...	...	...	...	...	...	...	...	...	...
	6554.24	1.44	−1.16	18.6	4.96	95.5	−0.11	86.6	−0.10	91.4	−0.01	103.3:	−0.55	109.2	−0.46	80.3	−0.51	23.7	0.19
	6556.08	1.46	−1.10	23.4	5.05	104.8	−0.11	96.8	−0.08	100.0	0.00	139.6:	−0.23	139.4	−0.21	94.0	−0.46	...	...
	6599.11	0.90	−2.06	9.8	4.99	85.3	−0.10	80.7	−0.01	75.9	−0.09	103.0:	−0.43	113.8	−0.28	90.9	−0.21	8.9	0.03
	6745.55	2.24	−1.10	4.1	4.94	32.2	−0.18	21.8	−0.32	25.9	−0.16	...	...	...	...	32.9:	−0.18	...	...
	7069.06	3.18	−0.27	6.5	5.23	23.1	−0.31	20.0	−0.33	31.7	−0.02	...	...	51.7:	−0.03	29.2	−0.21	5.1	−0.06
	7138.93	1.44	−1.72	7.2	5.01	74.0	0.01	65.2	0.01	64.8	0.02	103.9:	−0.09	...	...	65.6	−0.21	...	...
	7216.19	1.44	−1.30	22.6	5.17	110.3	−0.05	108.0	0.07	95.1	−0.09	118.3:	−0.50	...	...	123.4	−0.09	...	...
	7251.72	1.43	−0.86	36.7	5.03	127.8	−0.16	115.3	−0.16	128.2	0.09	149.9	−0.44	167.0	−0.25	120.5	−0.44	44.2	0.17
	7352.14	2.49	−0.83	2.3	4.63	21.1	−0.09	...	...	19.5	0.00	...	...	...	...	16.8	−0.21	...	...
	7357.74	1.44	−1.10	24.5	5.01	118.2	−0.01	113.1	0.08	...	...	128.4:	−0.43	138.4	−0.30	123.7	−0.14	23.2	0.03
	7364.11	1.43	−1.25	19.5	5.02	112.6	0.05	107.7	0.14	97.4	0.01	141.8	−0.15	151.1	−0.03	...	...	25.7	0.21
	7440.58	2.25	−1.08	10.3	5.33	60.1	−0.14	53.1	−0.15	...	...	86.7	−0.16	...	...	61.0	−0.21	...	...
	7580.28	2.23	−1.69	1.4	5.00	18.1	−0.03	15.2	−0.03	14.0	−0.01	...	...	27.3:	−0.06	...	...	...	...
	7949.15	1.50	−1.43	14.2	5.07	88.0	−0.12	71.8	−0.22	71.5	−0.21	...	...	117.1	−0.25	66.9:	−0.52	...	...
Ca I ...	6455.61	2.52	−1.50	57.4	6.46	137.7	−0.23	128.8	−0.17	114.4	−0.07	139.5	−0.42	155.7	−0.33	108.1	−0.44	66.0	0.12
	6464.68	2.52	−2.53	13.8	6.55	66.5	−0.08	56.5	−0.10	50.3	−0.08	72.4	−0.24	89.5	−0.08	47.2	−0.37	11.7:	−0.04
	6798.47	2.71	−2.72	9.0	6.70	44.6	−0.13	43.9	−0.04	32.2	−0.13	47.0:	−0.28	...	...	35.1	−0.19	...	...
Si I	7003.57	5.96	−0.86	61.1	7.58	32.5	0.21	26.0	−0.04	38.5	−0.06	...	...	...	...	11.3:	−0.93	63.0	0.02
	7005.90	5.98	−0.68	77.9	7.61	37.4	0.10	35.1	−0.06	43.8	−0.16	...	...	...	...	24.3	−0.72	76.5	−0.03
	7289.19	5.62	−0.62	98.0	7.54	51.9	0.00	67.4	0.08	64.4	−0.17	...	...	30.6:	−0.32	43.1	−0.74	99.9	−0.01
	7405.79	5.61	−0.57	91.9	7.41	50.7	0.06	59.4	0.06	62.3	−0.13	...	...	46.0	0.02	44.3	−0.65	111.6:	0.18
V I.....	6452.31	1.19	−0.98	8.5	4.13	52.1	−0.39	41.3	−0.47	57.2	−0.20	...	...	95.1:	−0.23	67.1	−0.33	...	...
	6605.92	1.19	−1.17	6.3	4.17	44.4	−0.38	37.1	−0.41	38.3	−0.37	...	...	73.5	−0.29	29.1:	−0.74	12.2:	0.39
Al I	6696.03	3.14	−1.65	40.7	6.62	84.2	−0.19	75.5	−0.23	78.3	−0.09	97.2	−0.22	97.5:	−0.22	87.5	−0.15	43.0:	0.06
	6698.67	3.14	−1.95	24.1	6.60	58.5	−0.15	57.3	−0.12	55.8	−0.07	55.7	−0.34	73.5	−0.14	45.1	−0.34	22.2	−0.01
	7632.29	4.02	−1.00	36.9	6.65	60.3	−0.19	67.0	−0.11	...	...	...	...	...	...	...	...	...	...
Y I.....	6435.05	0.57	−0.83	1.9	2.76	51.0	0.05	...	...	...	...	52.9:	−0.33	80.9:	−0.02	...	...	...	...
	6793.63	0.57	−0.24	14.4	3.11	...	...	...	...	...	...	...	...	...	...	...	...	21.1::	0.27
Mg I...	8712.69	5.93	−1.26	syn	7.66	syn	0.02	syn	0.00	syn	−0.08	...	...	syn	−0.18	syn	−0.63	syn	−0.03
	8717.82	5.93	−0.97	syn	7.60	syn	0.09	syn	0.02	syn	−0.02	...	...	syn:	−0.05	syn:	−0.62	syn	−0.06
	6318.71	5.11	−1.68	50.8	7.40	...	...	...	...	60.1	−0.21	...	...	81.5	0.12	55.3	−0.44	43.9:	−0.09
	7691.57	5.75	−0.78	126.1	7.66	...	...	...	...	...	...	...	...	68.0:	−0.47	61.5:	−0.84	107.1	−0.14
O I	7771.95	9.15	0.33	70.5	8.92	...	...	...	...	...	...	...	...	...	...	...	...	77.9	0.02
	7774.18	9.15	0.19	60.0	8.89	...	...	...	...	...	...	...	...	...	...	...	...	63.4	−0.02
	7775.40	9.15	−0.04	47.7	8.89	...	...	...	...	...	...	...	...	...	...	...	...	54.5	0.05

atlas. The line strengths are reported in Table 2. Not all lines could be measured in all stars due to differences in instrumental configuration, radial velocity shifts, cosmic-ray hits, and noisy line profiles. More uncertain measurements are marked with a colon.

Abundances were derived from the equivalent widths using an updated version of the LTE analysis package MOOG (Sneden 1973) and model atmospheres from the grids of R. L. Kurucz (1992, private communication). The van der Waals broadening was handled in the manner of Ünsold (1955) with an enhancement factor of 2.2, typical of the value found from and employed in solar and stellar analyses, applied to all species. The derived absolute solar abundance and normalized stellar abundance for each line are given in Table 1.

The λ8712 and λ8717 lines are the best Mg features in our spectra to derive Mg abundances. The former is particularly well blended in the Pleiades spectra with a neighboring Fe I line. Thus, Mg abundances were derived via spectral synthesis. The λ8700 line list was taken from the Kurucz CD-ROMs. The Pleiades and solar spectra show synthetic absorption in the region to be lacking since many observed features are not reproduced. However, we do not believe this introduces systematic error into our Mg abundances because reliable continuum windows seem to exist and because the absorption in the immediate Mg regions is dominated by absorption from a few stronger lines which are adjusted based on the solar spectra. The synthetic calculations were carried out in MOOG with instrumental broadening modeled by convolution with a Gaussian; rotational broadening was also included using the published $v \sin i$ values.

3.3. *Stellar Parameters and Uncertainties*

3.3.1. *Effective Temperatures and Microturbulent Velocity*

Initial estimates of the stellar $T_{\rm eff}$-values were taken from the photometric estimates in JSFS and Soderblom et al. (1999). Final values were determined spectroscopically by enforcing excitation balance (i.e., no trend of [M/H] vs. excitation potential) of the Fe I lines, the most numerous species in our analysis. Similarly, the microturbulent velocity was determined by the simultaneous requirement of no trend in the abundances with line strength; a solar value of 1.1 km s^{-1} was assumed.

The Ni I and Ti I lines in our spectra provided useful checks on the parameters derived from the Fe I lines. The adequacy of these procedures is indicated in Figure 1, which shows the abundance versus χ and reduced line strength for Fe I, Ni I, and Ti I lines in HII 676 after adjustment of the individual [Ni/H] and [Ti/H] values to the mean [Fe/H] by addition of a constant. The derived parameters are listed in Table 1.

By altering the assumed values of $T_{\rm eff}$ and ξ, trends can be introduced into the planes of Figure 1. Confidence levels of the resulting correlations are calculated from the correlation coefficients, yielding uncertainties in the parameters. We estimate the uncertainties in the microturbulence of $\lesssim$0.25 km s^{-1}. Uncertainties in the spectroscopic $T_{\rm eff}$-values are $\sim$75 K for the Pleiades stars and $\lesssim$90 K for the NGC 2264 stars; we conservatively adopt 90 K as the uncertainty for all of the latter.

The derived $T_{\rm eff}$-values for the two Pleiades stars are in fine agreement ($\pm$25 K) with the initial photometric estimates, suggesting no gross errors in the excitation analysis

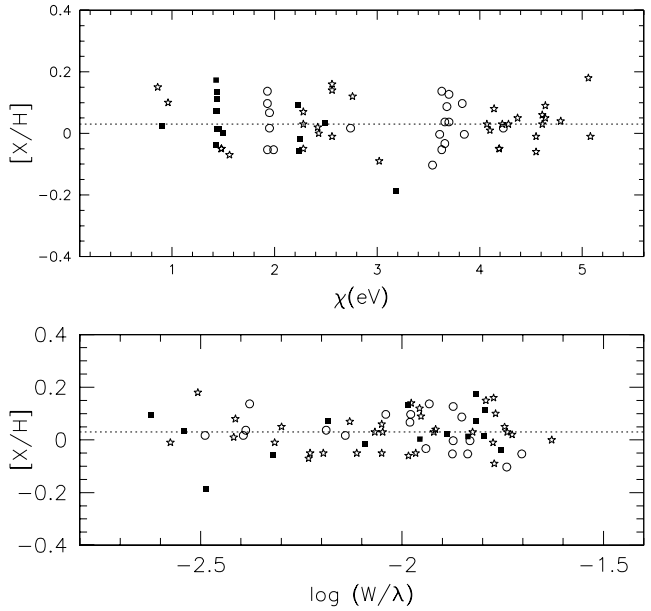

FIG. 1.—Top panel shows the line-by-line normalized abundances of Fe (*star symbols*), Ni (*open circles*), and Ti (*filled squares*) as a function of lower excitation potential for the Pleiades HII 676. The individual Ni and Ti abundance values have been adjusted to the mean [Fe/H] by addition of a constant. The bottom panel shows the line-by-line abundances vs. reduced line strength.

of these nearby zero-age main-sequence (ZAMS) stars. Similar agreement is seen for the probable NGC 2264 nonmember J1088, which we suspect is an early-type G interloping field dwarf. In contrast, we find $T_{\rm eff}$-values for J407, J428, J680, and J682 that are 201, 84, 228, and 522 K larger than the photometric estimates. On average, these differences are considerably larger than the errors in our spectroscopic determinations. Likely causes are underestimates in reddening (systematic or for particular stars), deviations in color-$T_{\rm eff}$ relations for some PMS stars, inadequacy in the model atmospheres, and excitation departures. Regardless, the differences underscore the uncertainty in PMS $T_{\rm eff}$ determinations (King 1998), which are critical to evaluating present-day Li abundances from the youngest stars. Given the $T_{\rm eff}$ revisions, we later present revised Li abundances in Table 5.

3.3.2. *Gravities and Model Metallicities*

The assumed overall metallicity of the model atmospheres is given in Table 1. These are very close to the final determined Fe abundances, but the effects on the derived abundances of modest departures from the assumed model metallicity are not great. We simply adopt a reasonable 0.15 dex uncertainty in the model atmosphere metallicity uncertainty when considering detailed errors.

A gravity of log $g = 4.60$ was assumed for both Pleiades stars on the basis of the binary star calibration shown in Figure 16.7 of Gray (1992) and theoretical isochrones. We believe this gravity accurate certainly within 0.15 dex (taken as the uncertainty) and probably less. For the warm NGC 2264 nonmember J1088, a gravity of log $g = 4.50$ was derived by forcing agreement between abundances derived from gravity-sensitive Fe II lines and those derived from the Fe I features; given the internal Fe abundance scatter and uncertainty in the other parameters, this estimate is accurate to within $\pm$0.25 dex. Ideally, gravities for the other

NGC 2264 stars would be similarly determined via ionization balance. Unfortunately, most of the Fe II lines in our wavelength region are high-excitation lines immeasurably weak in our cool star spectra. The two or three measurable lower excitation Fe II lines we could identify were noticeably blended in the Pleiades spectra and deemed unsuitable.

Thus, we have simply utilized the mass and radii values from the PMS theoretical models discussed in Soderblom et al. (1998) to estimate gravities for our NGC 2264 stars; these are given in Table 1. We have assigned a generous internal uncertainty of 0.50 dex to the theoretical gravities; although we believe the results to be more robust than this, this error also encompasses possible systematic errors. The log g–values are based on the photometric $T_{\rm eff}$ estimates adopted by Soderblom et al. (1998), and the detailed abundances given in Table 2 are calculated assuming no log g adjustment based on our refined spectroscopic $T_{\rm eff}$ estimates. The assumed gravity does not affect the derived parameters,[3] but does impact the abundances directly. The sensitivities to all parameters are given in Table 3, which gives our final results.

To consider systematic effects, revised log g–values were estimated from the PMS models assuming our hotter NGC 2264 $T_{\rm eff}$-values. The results are larger log g by 0.17, 0.09, 0.26, and 0.56 dex for J407, J428, J680, and J682. Even revisions of this magnitude do not seriously impact our results. For example, the most extreme revision is Δ[Si/H] = 0.15 dex for J682; changes with respect to Fe are smaller (even in this most extreme case Δ[Si/Fe] $\lesssim$ 0.09). Regardless, in Table 4 we list final mean abundances assuming both the adopted and revised gravities so that the systematic effects can be assessed.

3.4. *Blending and Line Identification Concerns*

Differential analyses of stars with parameters differing from the solar temperature and pressure may be complicated by variations in the strength of a blending feature contaminating a given line, e.g., a low-excitation line of moderate strength in a cool star may be considerably weaker in the hotter Sun. If such a feature was contaminated by an unrecognized high-excitation feature, the relative contribution of the high-excitation line to the blended line strength would be higher in the Sun; thus, one would erringly derive an underabundance in the cool star.

We have indeed observed such effects during our analysis. The low-excitation V I lines listed in Table 2 (and another V I feature, λ6504.2, not listed) yield low abundances with respect to Fe in our cool stars and a high abundance in the warm star J1088. A line list from the Kurucz CD-ROMs implicates high-excitation solar contaminants as the cause; while the Kurucz gf-values suggest that neighboring high-excitation features of Sc II, Ti I, Cr II, and V I have solar line strengths several orders of magnitude lower than the low-excitation λ6452.31 V I feature, a $\chi = 5.62$ eV Si I line at 6452.30 Å is of sufficient strength to affect the derived solar gf-values of Thévenin (1990) such that a $\sim$0.4 dex underestimate in [V/H] of our cool stars is the result. For the λ6605.92 V I line, we find a neighboring $\chi = 4.01$ eV Ti II feature at 6605.90 Å whose Kurucz gf-value (and a canonical solar Ti abundance) would result in a modified V I solar gf-value that yields—more in line with expectations—[V/H] $\sim$ 0.0 in, e.g., the cool Pleiades stars.

Another example is provided by the low-excitation ($\chi = 0.50$ eV according to Thévenin, 0.00 eV according to the Kurucz list) λ6687.51 Y I feature. Whereas our λ6435 Y I line gives a seemingly reasonable Pleiades abundance of [Y/H] = 0.05 for HII 676, the λ6687.51 line gives -1.01 in both HII 676 and HII 97. Whereas the Thévenin and Kurucz gf-values for the former line agree to within a percent, the gf-values for the latter feature differ by 1.5 orders of magnitude. This difference is again symptomatic of an errant solar gf-value due to a blend not affecting the Pleiades stars. Either of the neighboring $\chi = 4.14$ and 4.88 eV Fe I and Ca I features at 6687.49 and 6687.72 Å in the Kurucz line list provide the needed contamination to explain the discrepancy.

We estimate that such blends or incomplete solar line identifications may seriously afflict $\sim$25% of weak ($W \lesssim 15$

[3] Altering the assumed log g by a substantial 0.5 dex typically alters the derived microturbulence by $\sim$0.1 km s^{-1} and the inferred $T_{\rm eff}$ by 30–40 K.

TABLE 3

FINAL PLEIADES ABUNDANCES AND PARAMETER SENSITIVITIES

	HII 676			HII 97						
RATIO	Abundance	$\sigma_{\rm int}$ (dex)	$\sigma_{\rm tot}$ (dex)	Abundance	$\sigma_{\rm int}$ (dex)	$\sigma_{\rm tot}$ (dex)	$\Delta T_{\rm eff}$ ($^{+300}_{-200}$ K)	Δ log g ($\pm$0.25 dex)	$\Delta\xi$ ($\pm$0.5 km s^{-1})	Δ[m/H] ($\pm$0.1 dex)
[Fe/H]	0.04	0.01	0.07	0.08	0.02	0.08	$^{-0.01}_{+0.06}$	$\pm$0.03	$^{-0.08}_{+0.06}$	$\pm$0.04
[Ni/H]	$-$0.01	0.02	0.08	$-$0.03	0.02	0.08	$^{-0.04}_{+0.08}$	$\pm$0.04	$^{-0.08}_{+0.06}$	$\pm$0.04
[Ni/Fe].....	$-$0.05		0.03	$-$0.11		0.03				
[Cr/H]	$-$0.05	0.02	0.07	$-$0.09	0.06	0.09	$^{+0.15}_{-0.02}$	$\pm$0.00	$^{-0.05}_{+0.04}$	$\pm$0.03
[Cr/Fe].....	$-$0.09		0.05	$-$0.17		0.08				
[Ti/H].....	$-$0.09	0.02	0.09	$-$0.07	0.04	0.10	$^{+0.32}_{-0.15}$	$\pm$0.00	$^{-0.11}_{+0.09}$	$\pm$0.02
[Ti/Fe]	$-$0.13		0.09	$-$0.15		0.10				
[Ca/H]	$-$0.14	0.05	0.09	$-$0.09	0.05	0.09	$^{+0.29}_{-0.17}$	$\pm$0.04	$^{-0.06}_{+0.05}$	$\pm$0.02
[Ca/Fe]	$-$0.18		0.10	$-$0.17		0.10				
[Si/H]	0.10	0.05	0.10	0.03	0.04	0.10	$^{-0.25}_{+0.23}$	$\pm$0.07	$^{-0.01}_{+0.01}$	$\pm$0.02
[Si/Fe]	0.06		0.09	$-$0.05		0.09				
[Mg/H]	0.07	$\sim$0.08	0.11	0.03	$\sim$0.06	0.09	$^{-0.13}_{+0.16}$	$\pm$0.03	$^{-0.00}_{+0.01}$	$\pm$0.03
[Mg/Fe].....	0.03		0.10	$-$0.05		0.08				
[Al/H].....	$-$0.17	0.02	0.04	$-$0.15	0.05	0.06	$^{+0.13}_{-0.05}$	$\pm$0.00	$^{-0.03}_{+0.01}$	$\pm$0.01
[Al/Fe]	$-$0.21		0.07	$-$0.23		0.09				
[Y/H]	0.05	$\sim$0.10	0.16	...	...	...	$^{+0.45}_{-0.27}$	$\pm$0.00	$^{-0.14}_{+0.15}$	$\pm$0.01
[Y/Fe].....	0.01		0.16	...	...	...				

TABLE 4

NGC 2264 Abundances and Uncertainties

	J407			J428			J680			J682			J1088		
Ratio	Abundance	σ_{int} (dex)	σ_{tot} (dex)	Abundance	σ_{int} (dex)	σ_{tot} (dex)	Abundance	σ_{int} (dex)	σ_{tot} (dex)	Abundance	σ_{int} (dex)	σ_{tot} (dex)	Abundance	σ_{int} (dex)	σ_{tot} (dex)
[Fe/H]	−0.13 (−0.11)[a]	0.02	0.10	−0.28 (−0.27)	0.02	0.10	−0.14 (−0.11)	0.02	0.10	−0.67 (−0.60)	0.02	0.10	0.07	0.01	0.07
[Ni/H]	−0.19 (−0.16)	0.02	0.11	−0.33 (−0.32)	0.03	0.11	−0.25 (−0.21)	0.03	0.11	−0.78 (−0.69)	0.03	0.11	0.03	0.02	0.08
[Ni/Fe]....	−0.06 (−0.05)		0.04	−0.05 (−0.05)		0.04	−0.11 (−0.10)		0.04	−0.11 (−0.09)		0.04	−0.04		0.03
[Cr/H]	−0.05 (−0.05)	0.08	0.10	−0.19 (−0.19)	0.05	0.08	−0.15 (−0.15)	0.07	0.09	−0.27 (−0.27)	0.06	0.08	0.18	0.04	0.08
[Cr/Fe]....	0.08 (0.06)		0.11	0.09 (0.08)		0.09	−0.01 (−0.04)		0.11	0.40 (0.33)		0.10	0.11		0.04
[Ti/H]	−0.06 (−0.06)	0.03	0.11	−0.35 (−0.35)	0.06	0.12	−0.19 (−0.19)	0.05	0.12	−0.29 (−0.29)	0.05	0.12	0.07	0.04	0.09
[Ti/Fe]	0.07 (0.05)		0.13	−0.07 (−0.08)		0.14	−0.05 (−0.08)		0.14	0.38 (0.31)		0.14	0.00		0.06
[Ca/H]	−0.09 (−0.06)	∼0.07	0.15	−0.31 (−0.30)	0.07	0.15	−0.21 (−0.17)	∼0.10	0.16	−0.33 (−0.24)	0.09	0.16	0.04	∼0.07	0.09
[Ca/Fe] ...	0.04 (0.05)		0.13	−0.03 (−0.03)		0.13	−0.07 (−0.06)		0.15	0.34 (0.36)		0.14	−0.03		0.07
[Si/H]	−0.13 (−0.08)	0.03	0.17	...	...	...	−0.15 (−0.08)	∼0.10	0.20	−0.76 (−0.60)	0.07	0.19	0.04	0.06	0.08
[Si/Fe]	0.00 (0.03)		0.13	...	...	...	−0.01 (0.03)		0.16	−0.09 (0.00)		0.14	−0.03		0.08
[Mg/H] ...	−0.10 (−0.08)	0.07	0.12	...	...	...	−0.15 (−0.12)	0.14	0.17	−0.63 (−0.56)	0.09	0.13	−0.08	0.03	0.05
[Mg/Fe]...	0.03 (0.03)		0.09	...	...	...	−0.01 (−0.01)		0.15	0.04 (0.04)		0.11	−0.15		0.05
[Al/H].....	−0.08 (−0.08)	∼0.07	0.08	−0.28 (−0.28)	∼0.10	0.11	−0.18 (−0.18)	∼0.10	0.11	−0.25 (−0.25)	∼0.10	0.11	0.03	∼0.07	0.08
[Al/Fe]	0.05 (0.03)		0.12	0.00 (−0.01)		0.14	−0.04 (−0.07)		0.14	0.42 (0.35)		0.14	−0.04		0.08
[Y/H]	...	...	...	−0.33 (−0.33)	∼0.12	0.20	−0.02 (−0.02)	∼0.10	0.19	...	...	...	0.27	∼0.1	0.14
[Y/Fe].....	...	...	...	−0.05 (−0.06)		0.21	0.12 (0.09)		0.20	...	...	...	0.20		0.11
[O/H]	...	...	...	...	...	...	...	...	...	...	...	...	0.02	0.03	0.10
[O/Fe]	...	...	...	...	...	...	...	...	...	...	...	...	−0.05		0.15

[a] Values in parentheses are corresponding results assuming gravity revisions ($\Delta \log g = 0.17, 0.09, 0.26$, and 0.56 dex for J407, J428, J680, and J682) discussed in the text.

mÅ, say) low-excitation solar lines. Our results should not be greatly affected since most of the known cases we identified are limited to Thévenin's "case *b*" features, which are not relied upon heavily here; an exception is the apparently clean "case *a*" λ6793.6 Y I line which we found to yield [Y/H] $\lesssim -1$ in our cool NGC 2264 stars. Happily, miscreants can be efficiently identified and excluded by (*a*) noting their consistent effect on the abundances in different stars, (*b*) comparing the solar *gf*-values with Kurucz's *gf*-values, and (*c*) identifying specific blending features of sufficient wavelength and strength using the Kurucz line list.

A similar but opposite effect may exist for high-excitation lines in that low-excitation blends not affecting the solar *gf*-values or abundances may contaminate the cool Pleiades stars, resulting in derived overabundances. This problem is more insidious since it is not necessarily confined to the known-to-be-blended "case *b*" features. For example, we find the ($\chi = 5.86$) λ6848.57 Si I and ($\chi = 5.61$) λ7552.50 Ni I features to be high-excitation "case *a*" lines which yield huge overabundances ([*X*/H] = 0.5–0.6) in both Pleiades stars, apparently due to contamination by low-excitation blends not apparent in the solar spectrum. While our estimate is not necessarily robust or unbiased, our best guess is that perhaps as many as 15%–20% of the high-excitation lines could be noticeably affected by low-excitation blends in our cool Pleiades dwarfs. Fortunately, most of this minority fraction can be identified and excluded as described above.

4. RESULTS

Mean abundance ratios, [*X*/H] and [*X*/Fe], are listed for our Pleiades stars and NGC 2264 objects in Tables 3 and 4; V abundances are not included because they are deemed unreliable, and the Y results should be regarded with some caution since they are derived from a single line and suffer from lingering blending concerns. The tables list the mean *internal* uncertainty (σ_{int}) derived from the line-to-line scatter (assumed similar to the Fe or Ni results in those cases with few lines), followed by total mean uncertainties (σ_{tot}) which take into account the internal errors and the uncertainties in the parameters listed in Table 1. The final four columns of Table 3 list representative sensitivities to the parameters for our cool stars; these are not applicable to the considerably hotter J1088. The NGC 2264 abundance ratios that result from upward gravity revisions, discussed above, according to our spectroscopic T_{eff}-values are given in parentheses in Table 4.

5. DISCUSSION

5.1. *The Pleiades Results*

5.1.1. *Pleiades* Fe *Abundance and Comparison with Previous Work*

The mean Fe abundance from our two cool Pleiades stars is [Fe/H] = 0.06 with a total uncertainty of ∼0.05 dex. Potential systematic errors (continuum normalization, blending, model atmosphere adequacy) are more difficult to quantify, but we do not believe them to be large. The Fe analysis of two cool Hyades dwarfs by King & Hiltgen (1996) is very similar to the present one. Their value of [Fe/H] = 0.11 is in excellent agreement with the F and G star determinations of Cayrel, Cayrel de Strobel, & Campbell (1985) and Boesgaard & Friel (1990), who find mean values of [Fe/H] = 0.12 and 0.15; this agreement is encouraging considering the 1500–2000 K range in T_{eff} covered by the studies and the three different methods (photometric calibrations, Hα profile fitting, Fe I fine analysis) employed to determine T_{eff}.

Our Pleiades [Fe/H] falls between previous estimates derived from warmer stars. Boesgaard, Budge, & Ramsay (1988) studied 17 Pleiades F stars and determined a spectroscopic value of [Fe/H] = −0.03. Boesgaard (1989) selected the best eight stars and utilized new measurements of six Fe lines to find [Fe/H] = 0.02. Boesgaard & Friel (1990) analyzed new spectra for 12 of the same F stars and estimated [Fe/H] = −0.02. Cayrel, Cayrel de Strobel, & Campbell (1988) spectroscopically determined Fe abundances in four Pleaides G dwarfs; their mean abundance is [Fe/H] = 0.13.

Our Pleiades K dwarf–based value of [Fe/H] = 0.06 is intermediate to these F and G star estimates, and cannot be said to conflict with either given the mutual uncertainties. Placing 28 Pleiades F and G stars in the m_1 versus β plane, Eggen (1986) concluded that the Pleiades Fe abundance lies between an [Fe/H] of 0.0 and 0.1. His Stromgren calibration–based estimate of [Fe/H] = 0.08 is in fine agreement with our spectroscopic value. Nissen (1981) used Stromgren photometry and narrowband indices to find a mean [Fe/H] = -0.08 ± 0.04 for six Pleiades F stars, although two stars seem to have considerably lower abundances relative to the other four. The difference between the Eggen and Nissen results is mildly surprising since the former uses the photometric metallicity calibration of the latter.

5.1.2. *Abundances of Other Elements*

Derived abundance ratios (with respect to Fe) of other elements in our two Pleiades stars and the NGC 2264 objects are plotted versus atomic number in Figure 2. Fe, Mg, and Si are dominant contributors to free electrons in cool star photospheres. The Mg and Si abundances of our Pleiades stars appear to scale with the mildly enhanced Fe. From Table 3 we find mean values of [Mg/H] = 0.05 and [Si/H] = 0.07, again with a total uncertainty of ∼0.05 dex. Ni appears to be underabundant with respect to iron; our results suggest [Ni/Fe] = -0.08 ± 0.03. The similarity in the Ni and Fe line strengths, excitation distribution, ionization potential, and parameter sensitivities result in the small uncertainty in this ratio. Because of this, we tentatively conclude the slight underabundance is real; indeed, a similar Ni underabundance is found in all five NGC 2264 stars, too. If true, the Pleiades ratio would lie on the extreme edge of the disk field star distribution of Edvardsson et al. (1993). Excluding unknown systematic effects as the cause will require additional high-quality data; particularly valuable would be Pleaides stars near the solar T_{eff}.

Interestingly, the other light metals consistently show larger underabundances relative to Fe in both Pleiades stars. In contrast to Ni, this is not seen in our NGC 2264 stars. We find mean Pleiades values of [Cr/Fe] = -0.13 ± 0.06, [Ti/Fe] = -0.14 ± 0.07, [Ca/Fe] = -0.18 ± 0.07, and [Al/Fe] = -0.22 ± 0.06. Comparison with the numerous data from Edvardsson et al. (1993) indicates that these Pleiades stars' abundance ratios (particularly for Al and Ca) are remarkably low compared with field disk stars, especially when considered together. Again, identification of unknown systematic effects could come from detailed analyses of high-quality spectra of additional Pleaides stars.

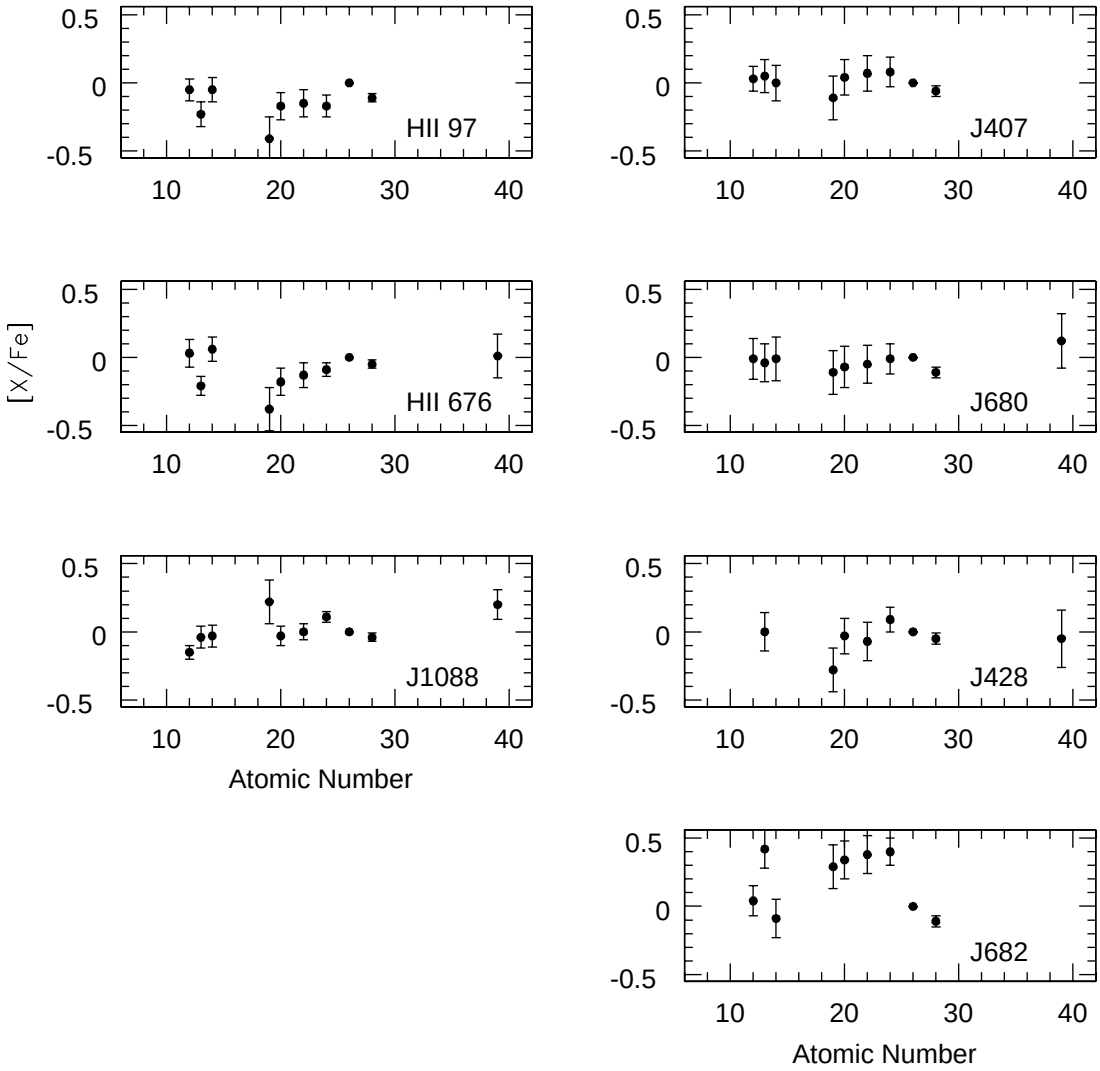

FIG. 2.—Abundance ratios (with respect to Fe) are plotted vs. atomic number for the two Pleiades stars and probable NGC 2264 nonmember (*left-hand column*) and the NGC 2264 PMS members (*right-hand column*).

There are several possible explanations for these odd ratios. First is Galactic chemical evolution. Cunha & Lambert (1994) find evidence of correlated B star O and Si abundance variations between Orion subgroups and suggest that these arise from variations in enrichment of the nascent gas by Type II supernovae (SN). This is not a likely explanation for our results given the differences between the α-element (Type II SN products) ratios: Mg and Si are more abundant than Ca and Ti. No simple signature of Galactic chemical evolution is reminiscent of our Pleiades abundance ratios.

Another possibility is circumstellar/interstellar chemistry. The elements Al, Ca, Ti, and perhaps Cr are often found to be considerably more depleted in the interstellar medium (ISM) than Fe, Mg, and Si. This pattern qualitatively mimics our photospheric abundances. Such a pattern might then be related to a disk/planet-star environment and/or photospheric accretion. Clearly, it would be of considerable interest to confirm the present results with additional data in more Pleiades stars.

A third possibility is ionization-related effects. The elements Mg, Si, Fe, and Ni have first ionization potentials ranging from 7.64 to 8.15 eV. Those for Al, Ca, Ti, and Cr are lower, ranging from 5.99 to 6.76 eV. Systematic errors in our analysis procedure that might lead to such an ionization-dependent effect are not apparent; moreover, this pattern is not seen in our NGC 2264 stars. We can only speculate that such a pattern might be introduced by, e.g., model atmosphere uncertainties, the presence of convective inhomogeneities, chromospheric effects, or other non-LTE (NLTE) effects. Such effects (whatever their cause) might have important consequences for the absolute and star-to-star abundances of Li, which has an even lower ionization potential of 5.39 eV.

To distinguish between the depletion and ionization possibilities, we present abundances of K in Table 5; K is useful in this regard since its interstellar depletion is comparable to or lower than that of Fe, Mg, and Si, but its ionization potential (4.34 eV) is even lower than that of Al, Ca, Ti, and Cr. These abundances are derived from the strong K I resonance line at 7699 Å; uncertainty in these abundances may arise from the lack of hyperfine structure information and NLTE effects. Excluding these, the total uncertainties in the individual K abundances are estimated to be $\sim$0.15 dex. The mean [K/H] ratio, -0.33 ± 0.10, is subsolar. Our suspicion is that lack of hyperfine structure and NLTE

TABLE 5

POTASSIUM, REVISED LITHIUM, AND OXYGEN ABUNDANCES

Star	Equivalent Width (K) (mÅ)	[K/H]	Equivalent Width (Li) (mÅ)	log N(Li) (LTE)	log N(Li) (NLTE)[a]	Equivalent Width (O I) (mÅ)	[O/H]
HII 676.....	486	−0.37	23	0.29	0.68	18.9/13.5/10.0	0.89/0.81/0.82
HII 97	447	−0.30	78	1.04	1.32		
GL 241						10.8/8.3/5.8	0.23/0.23/0.22
J407.....	287	−0.24	476	3.55	3.39	26.6/23.6/16.0	0.42/0.49/0.39
J428.....	394	−0.56	477	3.00	2.90	...	...
J680.....	605	−0.25	561	3.16	3.08	...	...
J682.....	305	−0.38	507	3.50	3.38	...	...
J1088	192	0.29	127	2.93	2.85	[b]	[c]
Sun	154	5.31[d]				[b]	[b]

[a] Calculated as in Soderblom et al. 1999; for the Pleiades stars, $T_{\rm eff} = 4500$, log $g = 4.5$, and [M/H] = 0.0 is assumed.
[b] See Table 2.
[c] See Tables 2 and 3.
[d] Absolute solar abundance, log N(K), derived with log $gf = -0.16$.

effects comparable to those of the analogous λ6707 Li I feature may lead to an *overestimate* of this value (perhaps by a few tenths of a dex).

The K abundances suggest an abundance pattern associated with ionization potential rather than interstellar depletion. If so, the similarities in the K I and Li I transitions, atomic data, and line strengths may mean that Li abundances could be afflicted too. More interesting is the possibility of star-to-star abundance variations. If the source of an ionization-dependent effect varies from star to star in the Pleiades, might this introduce related scatter in their Li (and K) abundances? This interesting question merits study of additional Pleiades stars and illustrates the potential utility of detailed abundances of numerous elements (not just Fe).

A fourth possibility is a temperature error ($T_{\rm eff}$ is 100 K too low, say) modestly larger than the estimated uncertainty. While such an error does not affect the mean [Fe/H] abundance, it does result in a suggestive concordance of the [Ni/Fe], [Cr/Fe], [Ti/Fe], [Ca/Fe], [Si/Fe], and [Mg/Fe] ratios at a value of −0.07 to within 0.03–0.04 dex. However, the [Al/Fe] and [K/Fe] ratios remain significantly lower at −0.18 and −0.30, respectively. In this case, plotting the revised abundance ratios in the various planes of Edvardsson et al. (1993) indicates the Pleiades stars re main consistently distinct from nearby field dwarfs.

Moderate $T_{\rm eff}$ adjustments are unable to remove the relative Al and K deficiencies and the differences with field dwarf abundance ratios that we find. Larger $T_{\rm eff}$ adjustments also fail to achieve simultaneous concordance, e.g., an upward adjustment of a few hundred degrees would alleviate the subsolar [Al/Fe] and [K/Fe] ratios but also introduce serious anomalies: [Ca/Fe] and [Ti/Fe] would approach 0.2 while the other α-element ratios [Mg/Fe] and [Si/Fe] would approach −0.25 as a result of their large and opposite temperature sensitivities. We note that $T_{\rm eff}$ adjustments are even more problematic in explaining an analogous abundance dichotomy in one of our NGC 2264 stars below. This does not mean that adjustments larger than our uncertainties are not at all possible—that is difficult to argue against definitively—rather, apparent curiosities remain after such adjustments.

5.1.3. *Comment on Intracluster Abundance Differences*

It is impossible to place meaningful limits on the internal Pleiades abundance scatter from two stars, but a couple of comments can be made. First, the agreement between our HII 676 and HII 97 abundances is outstanding. All the ratios agree to well within the uncertainties alone. The agreement seems considerably better than expected for 1 σ uncertainties, but it is not obvious that these have been overestimated.

Second, Cayrel de Strobel (1990) suggested that the Pleaides F and G star data indicate real star-to-star Fe variations. We do not believe this to be the case, however. The Pleiades F star Fe abundances of Boesgaard & Friel (1990) evince a scatter of 0.06–0.07 dex, which is actually smaller than their typical per star error of 0.09–0.10 dex. Similarly, the scatter in the G star Fe abundances of Cayrel et al. (1988) is 0.10 dex; again this is actually smaller than the typical ∼0.15 dex per star uncertainty listed in their Table 1.

Differing [Fe/H] values would alter a star's position in the cluster H-R diagram. Consider the case of HII 296 and HII 1776. Cayrel et al. (1988) determined [Fe/H] = 0.26 and 0.02 for these two Pleiades stars. The semiempirical and theoretical ZAMS fiducial and luminosity-metallicity sensitivity from VandenBerg & Poll (1989) and the two stars' $B-V$ indices predict a 0.62 V magnitude difference between the two stars if they have the same metallicity. If their true metallicities do differ by 0.24 dex, the predicted V magnitude difference is 0.25 mag. The observed magnitude difference is 0.55 mag, suggesting only a 0.05 dex [Fe/H] difference at most.[4] Evidence for an internal "metallicity" scatter in the Pleiades remains wanting.

5.1.4. *Abundances and the Pleiades Distance Modulus*

Pinsonneault et al. (1998) have considered the 0.3 mag discrepancy between the *Hipparcos* parallax-based Pleiades distance modulus and that inferred from cluster main-sequence fitting. They suggest the source of the discrepancy to be systematic errors at the 1 mas level in the parallaxes. As they note, another possibility is that the Pleiades metallicity is really a factor of ∼2 *lower* than previously believed. Our K star results suggest that this is not the case. Our Fe, Mg, and Si—the dominant electron donors in the stellar photosphere—abundances are slightly larger (by 0.06 dex) than solar.

[4] Unless the helium abundance of HII 296 was a very large $Y \sim 0.37$ compared to the canonical solar value of $Y \sim 0.27$.

5.1.5. Li *Abundance Scatter in Cool Pleiades Dwarfs*

Our two Pleiades stars' Li abundances presented in Table 5 (where we have remeasured the JSFS line strengths as part of this work) suggests a difference of ~ 0.65 dex. Their $T_{\rm eff}$ differs by 100–120 K, as inferred from both the photometry and excitation balance. From Figure 4 of JSFS we estimate the slope of the Li abundance decline with decreasing $T_{\rm eff}$ and find that the $T_{\rm eff}$ difference is consistent with only 0.2 dex of the Li abundance difference; thus, a real abundance difference of ~ 0.4 dex remains.

The source of such scatter in cool open cluster dwarfs is a long-standing problem of great interest and importance. Numerous mechanisms have been proposed to explain this scatter. An additional one—perhaps unpalatable but also unexplored—is the presence of intracluster abundance variations. As emphasized by Swenson et al. (1994), Li burning in cool dwarf models is a sensitive function of "metallicity," which (in this context) should not be identified with Fe abundance alone. We find no abundance differences between HII 97 and HII 676 that are significant with respect to the errors. However, it is also impossible to exclude small metal abundance differences of, e.g., 0.03 dex. As can be gauged from Figure 3 of CDP95, such a small difference can lead to large ~ 0.4 dex differences in standard model Li depletion at the age and temperature of our Pleiades stars.

Thus, very slight metal abundance differences could explain some or all of the Li abundance difference between HII 97 and HII 676. Exploring this possibility further would benefit from analysis of the slowly rotating Pleiades stars more amenable to accurate abundance analysis near 5100 K evincing a Li abundance spread $\gtrsim 1$ dex. At this $T_{\rm eff}$, the model predictions suggest that the observed Li abundance spread would require metallicity differences of ~ 0.25 dex. Variations of this size can be easily detected or excluded. The [Fe/H] scatter of $\lesssim 0.1$ dex inferred from combining our results with those of Boesgaard & Friel (1990) and Cayrel et al. (1988) argues, albeit indirectly, against a metal abundance scatter of this size as responsible for the Li spread.

As noted above, our abundances seemingly evince an ionization potential–related pattern. If real, this could have consequences for the Li abundances. Moreover, if such an effect varies from star to star, this may introduce scatter in the Li abundances. Relatedly, we note that Pleiades Li abundances and K line strengths show scatter significantly larger than measurement errors and that the star-to-star Li and K differences are correlated (King et al. 2000). This possibility could be explored with, e.g., additional Al determinations in Pleiades with a range of $T_{\rm eff}$. If the Al underabundance is a real signature of Galactic evolution, one expects a constant low abundance. If more speculative possibilities (circumstellar/interstellar chemistry or ionization) are correct, then Al might show star-to-star variations; of particular interest would be the extent of scatter above and below ~ 5200 K, the $T_{\rm eff}$ below which large variations in Pleiades Li become apparent.

5.2. *The NGC 2264 Results*

5.2.1. *J407, J428, and J680*

The mean Fe abundance for J407, J428, and J680 from Table 4 is [Fe/H] $= -0.18$ with a scatter of 0.08–0.09 dex, which is comparable to the estimated total uncertainties; the value assuming the revised gravities based on our spectroscopic $T_{\rm eff}$-values is little changed at -0.16. Like our Pleiades stars, these stars (and the other cool member J682) all evince a small Ni deficiency: [Ni/Fe] $= -0.08 \pm 0.03$; again, this is independent of the choice of log g.

The abundance ratios with respect to Fe of all other elements in all three stars, and thus their mean, are solar (i.e., to within a couple hundredths of a dex, $[X/{\rm Fe}] = 0$) within the uncertainties; again, this is independent of the adopted log g. Consistently low Al, Ti, and Ca abundances seen in our Pleiades are not evident for these NGC 2264 PMS stars.

J428 has an interesting pattern of abundances ($[X/{\rm H}]$) with respect to J407 and J680. All the elements in J428 are consistently ~ 0.15 dex lower than in the other two stars. The lower abundance also is seen for K, which is 0.3 dex lower in J428 relative to J407 and J680. The difference, then, does not seem to be due to chance. Table 4 shows that the difference does not depend on possible choices of log g. The parameter sensitivities given in Table 3 indicate that simple errors in $T_{\rm eff}$ or log g cannot simultaneously account for a uniform underabundance in all the elements, e.g., witness the difference in magnitude of $T_{\rm eff}$ sensitivity of Fe compared to Ti and Ca. The necessary underestimate in log g (~ 1.25 dex) to bring the Fe abundance into agreement with J407 and J680 is unrealistic.

A more realistic explanation is a plausible overestimate of the microturbulence which would lower all the abundances. This effect would be exacerbated as our iterative analysis would then adopt an errantly low model atmosphere metallicity which would lower all the abundances slightly further still. Another possibility is binarity. On the basis of our single epoch modest S/N spectrum it is difficult to exclude a blending SB2 component. The effects of dilution could errantly lower our measured equivalent widths, resulting in a derived underabundance. If so, though, we believe the effect to be considerably less than the maximum ~ 0.3 dex effect expected from an identical unblended companion. This is consistent with a mildly subsolar metal abundance.

At present, our best estimate from these stars is [Fe/H] $= -0.15$, a mild Ni deficiency [Ni/Fe] $= -0.08$ similar to that seen in our Pleiades stars, and solar ratios (with respect to Fe) of the remaining elements.

5.2.2. *The Probable Nonmember J1088*

Soderblom et al. (1999) ascribed ambiguous but probable nonmembership to J1088 on the basis of its Hα absorption, discrepant radial velocity, slightly low Li abundance, and color-magnitude diagram position. This classification seems confirmed by the abundances. All abundances except Mg are slightly supersolar, with [Fe/H] $= 0.07$. In addition, the spectroscopic gravity of log $g = 4.50$ is rather high and more consistent with a near-ZAMS classification; indeed, the Li abundance and gravity are even consistent with Hyades age values.

5.2.3. *Abundances in J682*

As seen in Figure 2, curious results are found for J682. Our derived Fe abundance of [Fe/H] $= -0.67 \pm 0.10$ is starkly lower than the other three cool members. Like the others, Ni shows a small deficiency of [Ni/Fe] $= -0.11 \pm 0.11$. The Si and Mg ratios with respect to Fe are solar within the uncertainties. However, the abundances of the remaining elements (Cr, Ti, Ca, and Al) are significantly higher at $[X/{\rm H}] \sim -0.29$. This dichotomy is analogous to

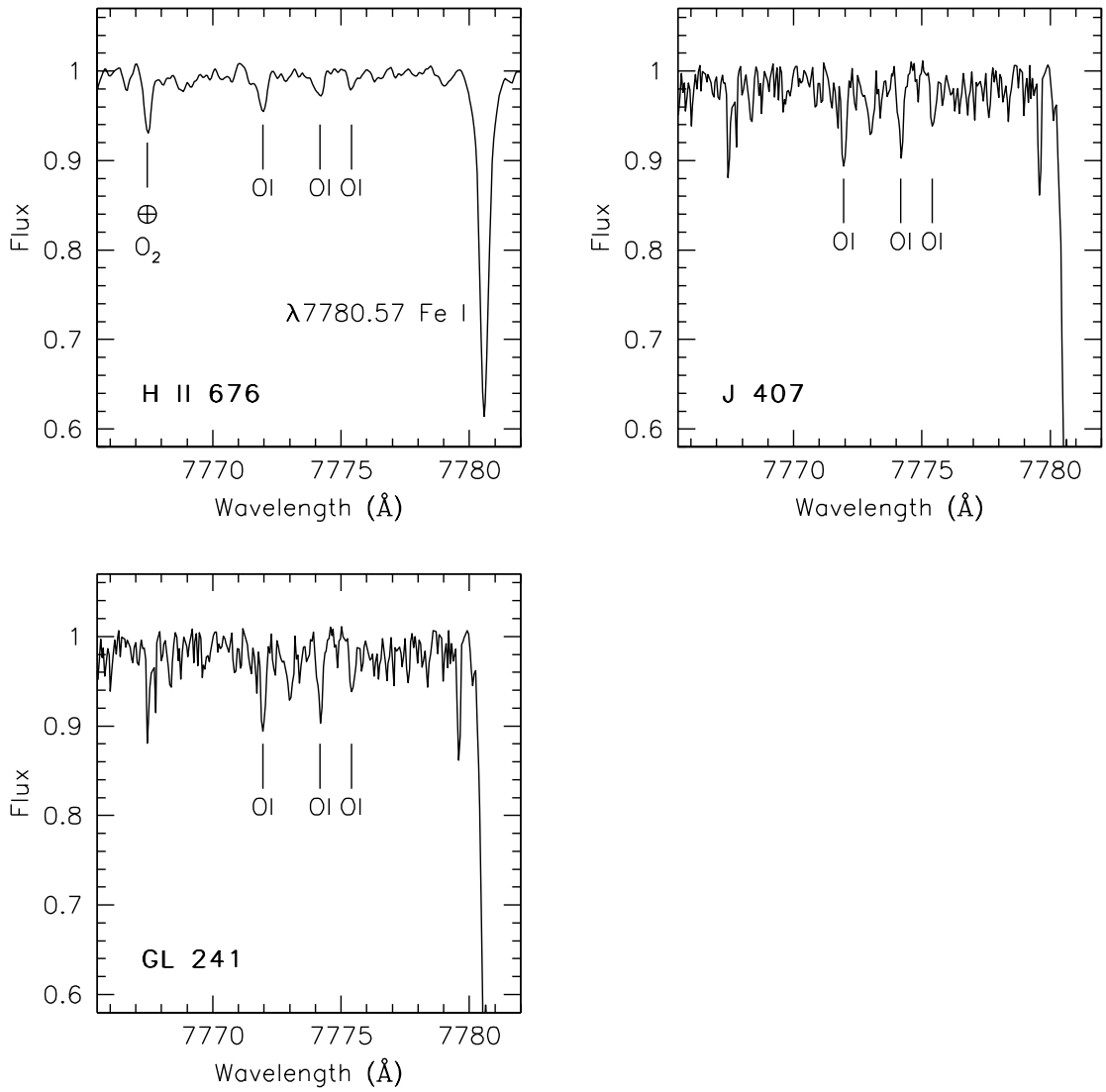

FIG. 3.—Spectrum of the λ7774 O I triplet region in our cool Pleiades HII 676, the cool PMS star NGC 2264 J407, and the older field K dwarf GL 241. The expected positions of the λ7774 O I triplet are marked. Each of these positions apparently corresponds to a real feature of significant strength and breadth in our spectrum of each star. The decreasing line strength from the blue line to the red line is also the behavior expected of the O I triplet.

that seen in our Pleiades stars, except more extreme and in the opposite sense with lower ionization potential elements showing higher abundances. Table 4 indicates that this is true regardless of which (substantially different) log g-value is adopted in the analysis.

Like our Pleiades stars, the source of the difference does not seem to reside in parameter errors. While the $T_{\rm eff}$ sensitivity of Fe, Ni, Si, and Mg is the same and opposite to that of Cr, Ti, Ca, and Al, no constant $T_{\rm eff}$ offset can bring all the abundances into agreement. In addition, any $T_{\rm eff}$ adjustment would have to be implausibly large ($\sim 10^3$ K) to bring just the Fe abundance into agreement with the other three NGC 2264 stars. The uncertainty estimates from the excitation balance analysis suggest considerably smaller values (± 90 K).

The photospheric abundance differences thus qualitatively mimic a pattern opposite to interstellar abundances but also could be interpreted as depending on ionization potential. Comparing the J682 K abundance in Table 5 with those of J407 and J680 suggests that the [K/H] and [K/Fe] ratios are more aligned with Cr, Ti, Ca, and Al rather than Fe, Ni, Mg, and Si; such alignment was inferred in our Pleiades stars, too.

Whatever the cause of these intraphotospheric and star-to-star differences, they raise concern about the reliability of LTE analyses with standard model atmospheres in PMS and active ZAMS stars. A particularly important question is how such deficiencies affect the derived absolute and star-to-star Li abundances in young clusters, which provide critical information concerning stellar physics and Galactic chemical evolution. Additional abundance determinations from high S/N and resolution spectroscopy of numerous elements in more young cluster stars spanning a large range ($\gtrsim 1000$ K) in $T_{\rm eff}$ are needed to investigate these important issues more substantively.

5.2.4. *Revised* Li *Abundances*

The revised Li abundances of our cool NGC 2264 stars presented in Table 5 are higher than those presented in Soderblom et al. (1999) as a result of our higher spectroscopic $T_{\rm eff}$ estimates. They noted evidence for star-to-star scatter in NGC 2264 Li, but believed it likely attributable to

uncertainties associated with the photometric temperatures. However, the spectroscopic $T_{\rm eff}$-based abundances seem to either exhibit a 0.20–0.25 dex scatter about a mean (NLTE) value of 3.19 or show a precipitous 0.4 dex drop over $\sim$300 K in $T_{\rm eff}$. If the former, then a conservative 0.15 dex estimate of the Li abundance uncertainty suggests a modest 0.15–0.20 dex real scatter. Regardless, either explanation would conflict with standard stellar models of uniform metal abundance, which are unable to produce such scatter or yield such a steep Li decline with $T_{\rm eff}$ at the young age ($\sim$5 Myr) of NGC 2264.

5.3. *Presence of the* O I *λ7774 Triplet*

Figure 3 shows our Keck spectra of HII 676 and J407 in the λ7774 O I triplet region. The expected positions of the O I triplet lines are marked. To within $\sim$0.05 Å, each position contains a feature which extends below the noisy pseudocontinuum and has significant breadth. Moreover, as commonly observed and expected from reasonably well-determined *gf*-values, the three features decline in strength from blue to red. The spectrum of HII 97 is similar in all respects. None of the other cool NGC 2264 stars studied here conclusively demonstrates the presence of the triplet, although the strongest bluest (7771.95 Å) component of the triplet may be marginally detected.

The presence of the lines in our two Pleiades stars and in J407 is remarkable. For solar [O/H], these particular features should be vanishingly weak in our spectra. As summarized in Table 5, however, the measured line strengths suggest a Pleiades O abundance enhanced by 0.85 dex over solar. The J407 abundance, [O/H] = 0.43, also represents a large overabundance. Figure 3 also contains a high S/N ($\sim$150) spectrum of the K6 field dwarf GL 241, which was obtained with the same instrumental configuration used in Fischer (1998). This inactive star has no measurable Li feature, suggesting a much greater age (a Gyr or more) than our NGC 2264 and Pleiades objects. The spectroscopic $T_{\rm eff}$ (4555 K) and Fe abundance (~ -0.10) are similar to our cluster stars (Fischer 1998). As can be seen, the O I triplet is evident in the older cool field dwarf. The line strengths suggest an abundance [O/H] $\sim$ 0.2 (Table 5; calculated assuming $\log g = 4.60$ and $\xi = 1.2$ km s^{-1}). NLTE effects are believed to affect abundances derived from the O I triplet in solar-type stars. However, at the solar $T_{\rm eff}$, gravity, and O abundance, the NLTE corrections are small (~ -0.06 dex; Takeda 1994) and *decrease* with decreasing $T_{\rm eff}$. Thus, the value in the K dwarf is surprising, suggesting either a genuine overabundance or shortcomings in the NLTE calculations.

Because the larger enhancements in our cluster stars seem exceedingly unlikely—particularly in light of the F and G star results of King (1993)—we can only speculate as to the cause. One possibility is additional unconsidered NLTE effects due to the presence of a strong chromosphere in our young stars. Recently, Takeda (1995) has shown that including the chromospheric temperature rise as part of model atmospheres can lead to significant NLTE effects on the formation of the O I lines *in the Sun*. Unfortunately, detailed NLTE line formation computations including the presence of chromospheric layers in model atmospheres appropriate for our cool stars have not been carried out. If such a mechanism is the root cause, it may be interesting that the overabundance in the older Pleiades stars is larger than the much younger NGC 2264 star.

The O I results demonstrate that LTE analyses with standard model atmospheres are inadequate for some transitions in some PMS and ZAMS stars. While such a general claim is not particularly surprising, detailed abundances of a variety of elements in numerous young cluster stars are sorely lacking. Thus, the extent to which related or unrelated systematic effects are important factors to consider in such stars remains poorly known. Such effects may have to be better understood before rigorously reliable absolute and relative abundances of important elements like Li can be derived with full confidence in young stars.

6. SUMMARY

We derive spectroscopic parameters and abundances of several elements in two cool Pleiades dwarfs, four cool NGC 2264 PMS stars, and a probable NGC 2264 nonmember from high-resolution, moderate S/N, Keck/HIRES spectra. The NGC 2264 abundances are some of the first for elements other than Fe and Li in PMS stars. Our modest-sized sample was selected to minimize potential sources of error and uncertainty. Particular attention was paid to blending concerns.

Our Pleiades Fe abundance, [Fe/H] = 0.06 $\pm$ 0.05, is between spectroscopic values from F and G stars and in satisfactory agreement with photometric estimates. The concordance of spectroscopic values is quite reasonable given the range in $T_{\rm eff}$, the differing model atmospheres employed, and the different means (photometric, Balmer profiles, Fe I fine analysis) by which $T_{\rm eff}$-values have been estimated. Our abundance does not resolve the 0.3 mag discrepancy in the Pleiades distance modulus derived from main-sequence fitting and *Hipparcos* parallaxes. Mg and Si also show similar mild enhancements, but we find a small Ni deficiency ([Ni/Fe] = -0.08 ± 0.03) in both Pleiades and all our NGC 2264 stars; given the internal uncertainties and the similarity in the parameter sensitivities of Ni and Fe, we tentatively conclude the difference is real.

The Pleiades ratios of Cr-Ti-Ca-Al are significantly lower ([X/Fe] ~ -0.17); this pattern mimics that of ISM abundances. While the sensitivity of the Cr-Ti-Ca-Al abundances to $T_{\rm eff}$ is opposite to that of Mg, Si, Fe, and Ni, no simple adjustment in $T_{\rm eff}$ can bring all the results into simultaneous concordance. The low K abundances suggest the pattern is more closely associated with ionization potential; such effects might be related to the Pleiades Li scatter, but this is unclear. Various evidence suggests real intracluster [Fe/H] scatter is $\lesssim$0.05–0.10 dex; however, a small 0.03 dex [Fe/H] difference can explain the 0.4 dex Li abundance difference between our two cool Pleiades stars via the metallicity sensitivity of standard PMS Li burning. Investigating intracluster metal abundance differences as the source of Pleiades Li abundance scatter would best be accomplished by analyses of low $v \sin i$ Pleiades stars near 5100 K, where larger and easily detectable metal abundance differences are required to explain the Li scatter.

Three NGC 2264 members provide our best estimate of [Fe/H] = -0.15; except for Ni, the abundance ratios of the remaining elements are solar in these stars. The abundances in J428 are consistently 0.15 dex lower than in J407 and J680. Whether this is a real difference or due to plausible errors in the derived microturbulence, assumed model atmosphere metallicity, and/or spectral dilution from a SB2 component is unclear.

Mildly supersolar abundances for another NGC 2264

star (J1088) are consistent with its probable nonmembership (Soderblom et al. 1999). The fourth NGC 2264 member (J682) exhibits curiously low abundances ($[X/H] \sim -0.7$) of Mg-Si-Fe-Ni, but its Cr-Ti-Ca-Al abundances are ~ 0.3 dex larger. This dichotomy is in the opposite sense to that of the Pleiades stars. The star's K abundance is also aligned with its Cr-Ti-Ca-Al values, again suggesting a relation to ionization potential.

A 0.15–0.20 dex scatter or steep decline with $T_{\rm eff}$ is present in the NGC 2264 Li abundances rederived using our $T_{\rm eff}$-values; neither can be accommodated by extant stellar models. Finally, we note the surprising presence of the λ7774 O I triplet in our Pleiades stars, one of the cool NGC 2264 stars, and the K6 field dwarf GL 241. The inferred LTE O abundances are enhanced over solar by 0.23–0.85 dex, suggesting that even NLTE calculations of the O I triplet are incomplete and perhaps implicating the importance of an overlying chromosphere on line formation in cool young stars. The results demonstrate the potential utility of cluster abundances besides Fe and Li in addressing fundamental issues concerning stellar evolution and systematic errors in the analysis of cool PMS and ZAMS stars with the assumptions of standard model photospheres and LTE.

The observations were made at the W. M. Keck Observatory, which is operated as a scientific partnership between the California Institute of Technology and the University of California, and made possible by the generous financial support of the W. M. Keck Foundation.

REFERENCES

Boesgaard, A. M. 1989, ApJ, 336, 798
Boesgaard, A. M., Budge, K. G., & Ramsay, M. E. 1988, ApJ, 327, 389
Boesgaard, A. M., & Friel, E. D. 1990, ApJ, 351, 467
Cayrel, R., Cayrel de Strobel, G., & Campbell, B. 1985, A&A, 146, 249
———. 1988, in The Impact of Very High S/N Spectroscopy on Stellar Physics, ed. G. Cayrel de Strobel & M. Spite (Dordrecht: Kluwer), 449
Cayrel de Strobel, G. 1990, Mem. Soc. Astron. Italiana, 61, 613
Chaboyer, B., Demarque, P., & Pinsonneault, M. H. 1995, ApJ, 441, 876 (CDP95)
Chang, T. N., & Tang, X. 1990, J. Quant. Spectrosc. Radiat. Transfer, 43, 207
Cunha, K., & Lambert, D. L. 1994, ApJ, 426, 170
Demarque, P., Green, E. M., & Guenther, D. B. 1992, AJ, 103, 151
Edvardsson, B., Andersen, J., Gustafsson, B., Lambert, D. L., Nissen, P. E., & Tomkin, J. 1993, A&A, 275, 101
Eggen, O. J. 1986, PASP, 98, 755
Fischer, D. 1998, Ph.D. thesis, Univ. California, Santa Cruz
Fitzpatrick, M. J., & Sneden, C. 1987, BAAS, 19, 1129
Gray, D. F. 1992, The Observation and Analysis of Stellar Photospheres (Cambridge: Cambridge Univ. Press)
Jones, B. F., Shetrone, M., Fischer, D., & Soderblom, D. R. 1996, AJ, 112, 186 (JSFS)
King, J., Krishnamurthi, A., & Pinsonneault, M. H. 2000, AJ, 119, 859
King, J. R. 1993, Ph.D. thesis, Univ. Hawaii
———. 1998, AJ, 116, 254
King, J. R., & Hiltgen, D. D. 1996, AJ, 112, 2650
King, J. R., Stephens, A., Boesgaard, A. M., & Deliyannis, C. P. 1998, AJ, 115, 666
Kurucz, R. L., Furenlid, I., Brault, J., & Testerman, L. 1984, Solar Flux Atlas from 296 to 1300 nm (NSO Atlas No. 1; Sunspot: NSO)
Nissen, P. E. 1981, A&A, 97, 145
Pinsonneault, M. H., Stauffer, J., Soderblom, D. R., King, J. R., & Hanson, R. B. 1998, ApJ, 504, 170
Randich, S., Aharpour, N., Pallavicini, R., Prosser, C. F., & Stauffer, J. R. 1997, A&A, 323, 86
Sneden, C. 1973, ApJ, 184, 839
Soderblom, D. R., King, J. R., Hanson, R. B., Jones, B. F., Fischer, D., Stauffer, J. R., & Pinsonneault, M. H. 1998, ApJ, 504, 192
Soderblom, D. R., King, J. R., Siess, L., Jones, B. F., & Fischer, D. 1999, AJ, 118, 1301
Swenson, F. J., Faulkner, J., Iglesias, C. A., Rogers, F. J., & Alexander, D. R. 1994, ApJ, 422, L79
Takeda, Y. 1994, PASJ, 46, 53
———. 1995, PASJ, 47, 463
Thévenin, F. 1990, A&AS, 82, 179
Twarog, B. A., Ashman, K. M., & Anthony-Twarog, B. J. 1997, AJ, 114, 2556
Ünsold, A. 1955, Physik der Sternatmospharen (Berlin: Springer)
VandenBerg, D. A., & Poll, H. E. 1989, AJ, 98, 1451